

### Available online at www.sciencedirect.com



Nuclear Instruments and Methods in Physics Research A 498 (2003) 220-230

NUCLEAR
INSTRUMENTS
& METHODS
IN PHYSICS
RESEARCH
Section A

www.elsevier.com/locate/nima

# A high-energy (35–500 MeV) proton monitor for the Gravity Probe-B Mission

Susan McKenna-Lawlor<sup>a,\*</sup>, Peter Rusznyak<sup>a</sup>, Sasha Buchman<sup>b</sup>, Paul Shestople<sup>b</sup>, John Thatcher<sup>c</sup>

Space Technology Ireland, Ltd., National University of Ireland at Maynooth, Co. Kildare, Ireland
 W.W. Hansen Laboratory, Stanford University, CA, USA
 Cockheed Martin Missiles and Space, Palo Alto, CA, USA

Received 8 October 2002; accepted 22 October 2002

#### Abstract

An innovative fault tolerant, high-energy particle monitor designed to record protons in the range 35–500 MeV when in polar orbit aboard NASA's Gravity Probe B spacecraft, is described. This device, which is configured to provide continuous, reliable operation in the hostile particle environment traversed by the spacecraft, can potentially be used either as an onboard monitor or as a scientific experiment.

© 2003 Elsevier Science B.V. All rights reserved.

PACS: 20-29.40 Wk

Keywords: Solid-state detectors; Relativistic protons; Electrons

## 1. Introduction

1-628-6470.

NASA's Gravity Probe B (GPB) Mission is designed to study accumulated pointing errors in the axes of a set of four precision gyroscopes in the Earth's gravitational field with a view to establishing if a component of these errors can be attributed to the warping of space time and to the "frame dragging effect" (predicted by Einstein's *General Theory of Relativity*). Due to the extreme accuracy required, the observations need to be corrected for a number of potential sources of measurement errors, in particular, charging and

E-mail address: stil@may.ie (S. McKenna-Lawlor).

heating of the surfaces of the gyroscopes due to ambient, high-energy, proton fluxes.

A force modulation technique allows measurements to be made of gyroscopic charge to an accuracy of about  $10^{-13}$  C, while bipolar charge control to the same level of accuracy is achieved through utilising electrons generated by UV photo-emission. By suitably exploiting information supplied by an onboard High Energy Proton Monitor (EPM), operating in the energy range 35–500 MeV, the duty cycle of the charge control system can be maintained to better than  $10^{-3}$  C. Excessive heating of the gyroscopes is prevented through the ongoing process of black-body radiation (the thermal emissivity of the external coating of the superconducting gyroscopes is  $\sim 3-5\%$ ).

<sup>\*</sup>Corresponding author. Tel.: +353-1-628-6788; fax: +353-

Table 1
Technical specification of the Energetic Proton Monitor (EPM)

reclinical specification of the Energetic Froton Monitor (EFM)			
Power	3.5 W		
Mass:	3.5 kg		
Volume	$150\times150\times105\text{mm}$		
Science data rate	80 bit/s		
Time resolution	Programmable, 12.8 s default		
Energy resolution	$2 \times 16$ proton channels, configurable		
Measurement range	35–500 MeV protons		
Configuration	Two orthogonal proton telescopes		

# 2. The technical challenge

Measurement of  $\Delta E$  losses near the top of the EPM measurement range (500 MeV) challenges the limits of technical feasibility since this value is comparable with the theoretical noise floor determined by the solid-state detectors and their accompanying Charge-Sensitive Amplifiers (CSAs).

Table 1 provides a summary of the technical specifications of the GPB/EPM. The energy resolution is software configurable and can potentially provide a channel resolution of 256 (with maximum measurement resolution <0.5 MeV at the bottom of the range). To reduce the data rate of the instrument, the 256 PHA channels are, in practice, limited to 16 programmable science channels. The integration time is configurable from 100 ms upwards. Integral event channels are provided for each detector to allow dead-time correction to be made on the ground.

In what follows, Section 3 describes the particle radiation hazard along the GPB trajectory, Section 4 provides an overview of the EPM detector system, Section 5 outlines the electronic design, Section 6 the software design, Section 7 the Ground Support Equipment and calibration of the instrument. Section 8 contains general concluding remarks.

# 3. Radiation hazard

The main components of the Earth's proton radiation environment are made up from (1) Galactic Cosmic Rays; (2) particles trapped in

the Geomagnetic Field (forming the Van Allen Radiation Belts) and (3) particles accelerated in association with solar activity. Fig. 1 presents typical energy spectra of these different populations in the Earth's magnetosphere (E. Daly, private communication).

Because the centre of the Earth's magnetic dipole is displaced with respect to the centre of the Earth, the fluxes of trapped particles are larger at low latitudes (a few hundred kilometres) over the South Atlantic Ocean than anywhere else at the same altitude. This results in the formation of a local particle enhancement above Brazil known as the South Atlantic Anomaly (SAA). Due to the heating and expansion of the atmosphere during periods of high solar activity, proton fluxes in the SAA are less at low altitudes during solar minimum than during solar maximum (reflecting the 11-year cycle).

Fig. 2 shows a world map of satellite locations where Single Event Upsets (SEUs) were recorded aboard a polar orbiting satellite at 700 km [1] Two features are especially apparent, namely the strong clustering of upsets in the SAA and the preferential distribution of the remaining upsets at high latitudes. These latter upsets were triggered by galactic cosmic rays and by solar related events which were partially prevented from reaching lower latitudes because of geomagnetic shielding. The high inclination of GPB in its polar orbit results in that spacecraft being exposed to proton radiation during an appreciable fraction of its trajectory since, close to the polar regions, the Earth's magnetic field funnels protons down towards the magnetic poles. The scheduled launch of GPB is in the closely post-maximum phase of sunspot cycle 23 when, based on the experience of previous cycles, especially energetic solar related proton events can be expected [2]. This makes the onboard monitoring of energetic particle events essential to the successful realisation of the scientific aims of the mission.

# 4. Detector system

Energetic charged particles can be detected using solid-state silicon detectors. These constitute

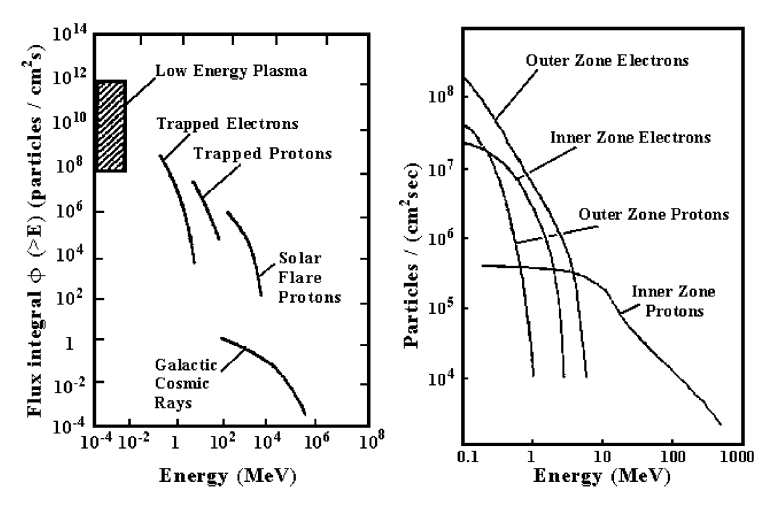


Fig. 1. Typical energy spectra of the major populations of energetic particles in the Earth's magnetosphere (left) and typical energy spectra of ions and electrons trapped in the inner and outer radiation belts (right) (E. Daly, private communication).

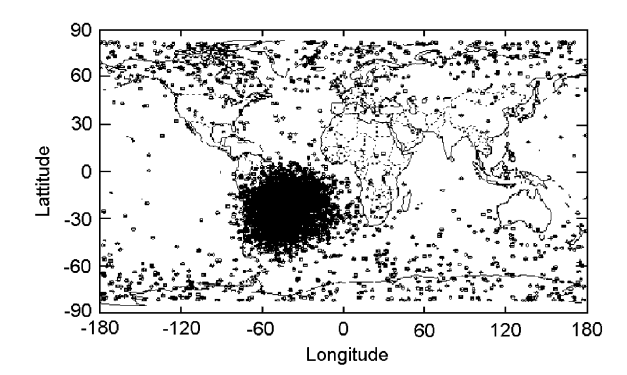


Fig. 2. World map of satellite locations where SEUs were recorded by UoSAT along a polar orbit (700 km).

in practice large, reverse biased, silicon diodes that act as miniature ionisation chambers. The charged particles that impact on these detectors loose their energy through the creation of electron—hole pairs inside the silicon wafer. If the reverse bias voltage applied creates a large enough electrical field, these charge carriers do not recombine but drift instead towards the electrodes, where they deposit an amount of charge that is directly proportional to the energy lost by the particle inside the detector.

This charge can be converted to a shaped, unipolar, pulse using a Charge Sensitive Preamplifier (CSA). The amplitude of the pulse is, for any pulse shaping time constant, directly

proportional to the charge collected at the electrode and also, therefore, directly proportional to the energy lost by the original particle. Through connecting a suitable Pulse Height Analyser (PHA) at the output, the energy loss concerned can be determined to a required resolution.

Although this method works very well for detecting low-energy charged particles, the problem encountered in the case of highly energetic protons is that they penetrate the silicon substrate and, therefore, do not loose all their energy inside the detector. However, the energy loss remains proportional to the incoming energy although linearly, not inversely. A hyperbolic energy loss curve is displayed in Fig. 3, which shows that the maximum energy a proton may loose in a 700 μm silicon detector behind a 3 mm tantalum shield is ~8 MeV. A proton with higher incoming energy will penetrate the detector and, in consequence, will loose less energy than this. As the incoming energy increases, the energy lost inside the detector becomes yet less, approaching, so-called, "minimum ionisation" (which is approx. 250 keV in the configuration discussed above).

Given that the energy loss characterising penetrating protons is inversely proportional to their incoming energies, it is possible to analyse protons having significantly higher energies than those monitored using only the stopping power of the

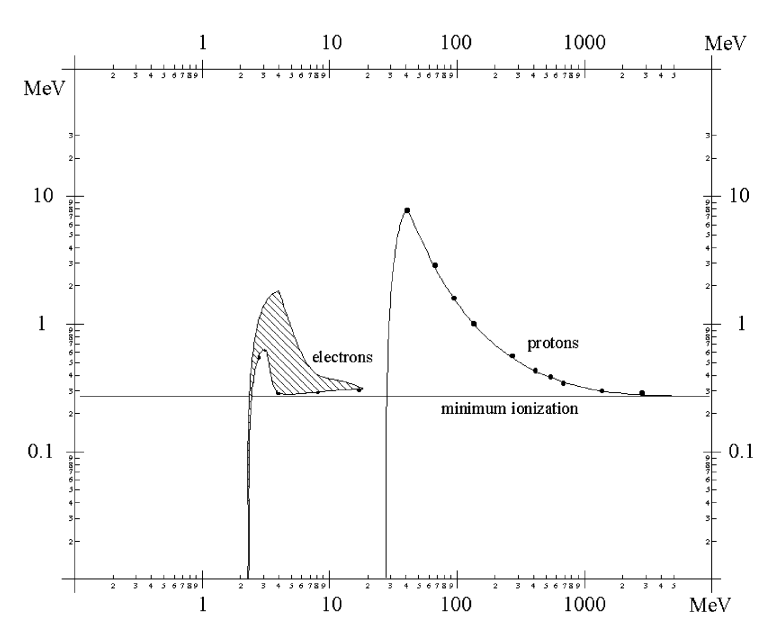


Fig. 3. Energy loss curves for protons and electrons in a 700 µm silicon detector behind a 3 mm tantalum shield.

detector. In order to distinguish between penetrating and stopped protons (as a low-energy proton that is stopped inside the detector may loose precisely the same energy as a penetrating particle of much higher energy), a thin silicon detector is installed behind the thick one. The signal from this latter detector is considered in association with the signal produced by the thick detector and the PHA is only enabled if these two event detection signals follow each other closely in time (i.e. form a coincidence).

Another problem encountered when detecting high-energy protons is the presence of energetic electrons. In the Earth's radiation environment where Gravity Probe B will fly, especially inside the SAA, various species of charged particles are present. There is, in particular, in the relevant region a significantly larger trapped electron than a trapped proton population. These trapped electrons display energies up to approx. 3-4 MeV. For the present application we wish to analyse only solar protons and electron detection is deemed to constitute a contamination of the proton monitoring process. However, as can be seen in Fig. 3, certain penetrating electrons of relatively low energies may loose the same energy inside the thick detector as is lost by solar protons. Also, energetic electrons loose more energy than might initially be expected, due to the fact that they do not follow a straight line inside the detector. If they did so, their energy loss would approach the bottom curve of the hatched area. The energy loss indicated in Fig. 3 for electrons is only an approximation, provided to demonstrate the problem of detecting protons in an environment contaminated by electrons.

To exclude electron events from the measurements, two thin front detectors (each of  $150\,\mu m$ ) are added to the detector sandwich (see Fig. 4). Since, as already mentioned, electrons do not follow a straight line, they tend to loose significantly different energies inside the two front detectors. By introducing a differential amplifier for the two front detectors which drives a programmable threshold discriminator, it is thus possible to determine from the response whether a given particle is an electron or a heavier particle.

We can then exclude the vast majority of electron events and achieve quasi-electron-free high-energy proton measurements simply through only enabling the PHA if the energy loss difference between the two front detectors is not more than, say, 60 keV (the value chosen is software programmable), given also that the coincidence criterion is

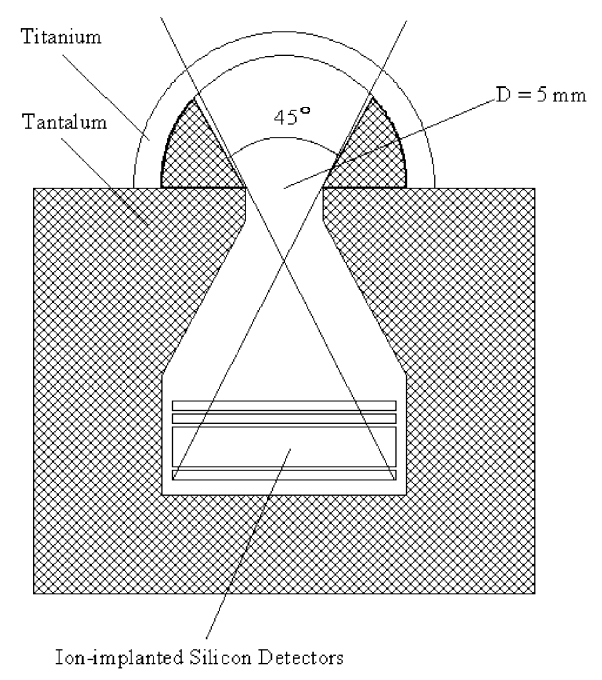


Fig. 4. Schematic diagram of the proton telescope of the EPM.

met (i.e., that the particle penetrates the thick detector and enters the back detector).

Overall, the detector system consists of four, ion-implanted, silicon detector layers, stacked as shown in Fig. 4. The surface of the detector stack is completely covered by a dome-shaped titanium shield (3 mm thick), which sets the lower energy threshold of the device at  $\sim 35$  MeV. To reduce the effect of stray particles, the detector sandwich is mounted inside a 2 mm thick tantalum enclosure located within an enveloping aluminium structure.

The EPM has two integral channels for electron events > 3 MeV: a > 500 MeV proton channel and an alpha particle ( $\alpha$ ) channel The  $\alpha$  measurement is based on the fact that, while protons may not loose more than  $\sim 9$  MeV in detector 3, heavier particles, naturally, loose more energy than this, and so can be identified. The lower threshold for  $\alpha$  particles (determined by the titanium shield and the coincidence criterion) is approx. 150 MeV.

The detection efficiency of the Detector System for protons is shown in Fig. 5.

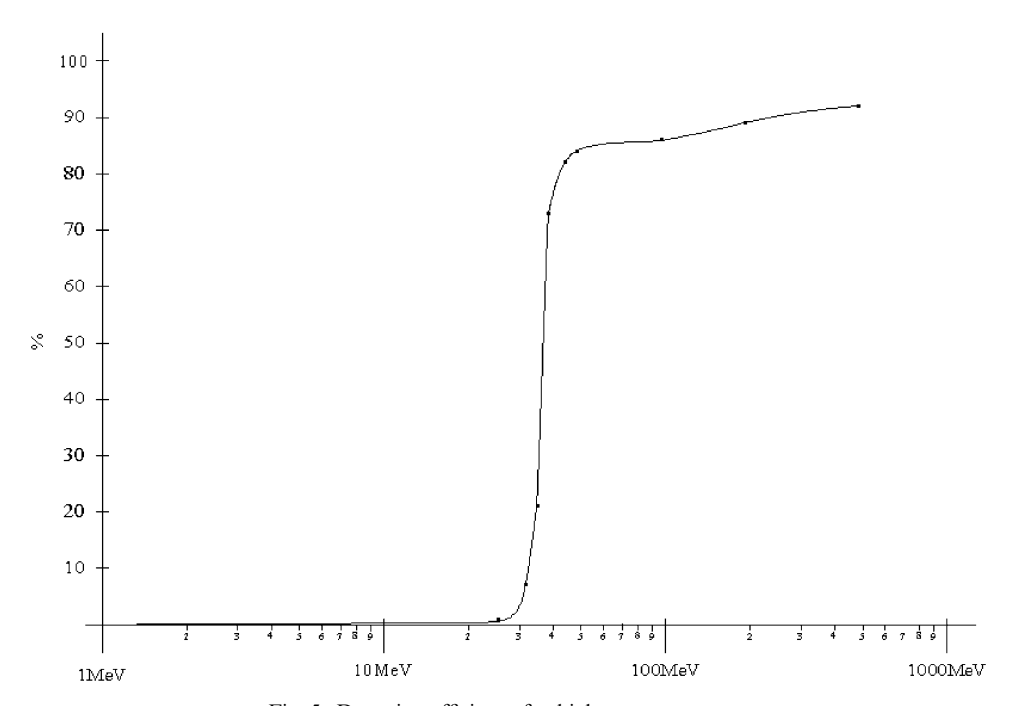


Fig. 5. Detection efficiency for high-energy protons.

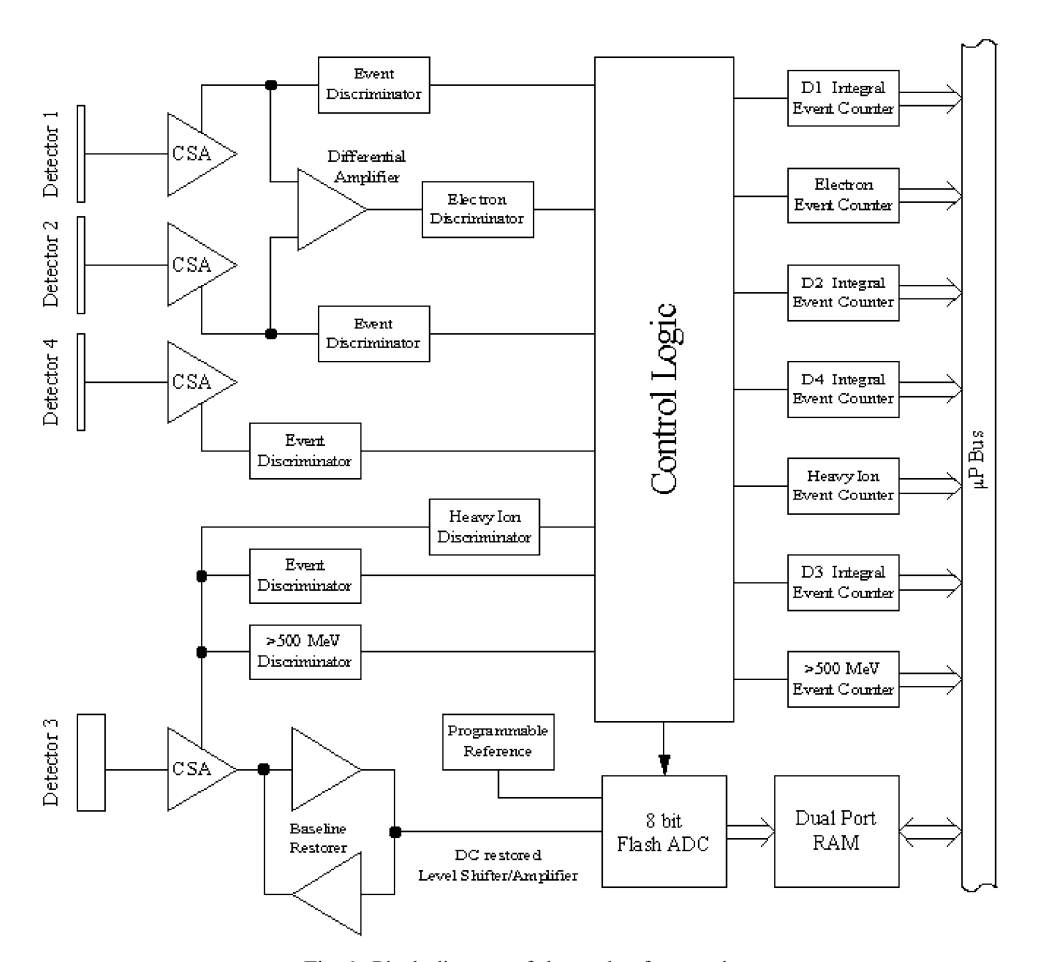


Fig. 6. Block diagram of the analog front end.

# 5. Electronic design

The block diagram of the analog front end for one telescope is displayed in Fig. 6 (the second telescope has identical electronics). The CSAs selected are AMPTEK A225 s. This is an ultralow noise, low power, large dynamic range device which contains Pulse Shaping Amplifiers (featuring a 2 ms time constant with pole-zero cancellation). This shaping time constant limits the maximum speed of the analyser to approx.  $50 \operatorname{stochastic} k$ -events/s/telescope. The proton event detection is, however, significantly faster (based on a  $500 \operatorname{ns}$  shaping time constant), and it reaches  $\sim 200-300 k$ -events/s. The event detection circuitry is used for the control logic and it is also connected to the integral event counters.

In addition to the PHA, integral event counters are provided for each detector in both telescopes. These integral channels (see above) allow the onboard software to correct for the dead time associated with the analog processing of events (primarily using the gated baseline restorer). The dead time is fixed at 15 µs/event.

A detailed block diagram of the analog frontend serving the two front detectors is provided in Fig. 7. The main function of this circuitry is to suppress electron detection and, thus, provide 'clean' proton measurements.

For energy loss measurements, a 700 µm ionimplanted silicon detector is employed (for GPB two identical telescopes are mounted in an orthogonal arrangement). The energy loss is analysed using a 256 channel Pulse Height

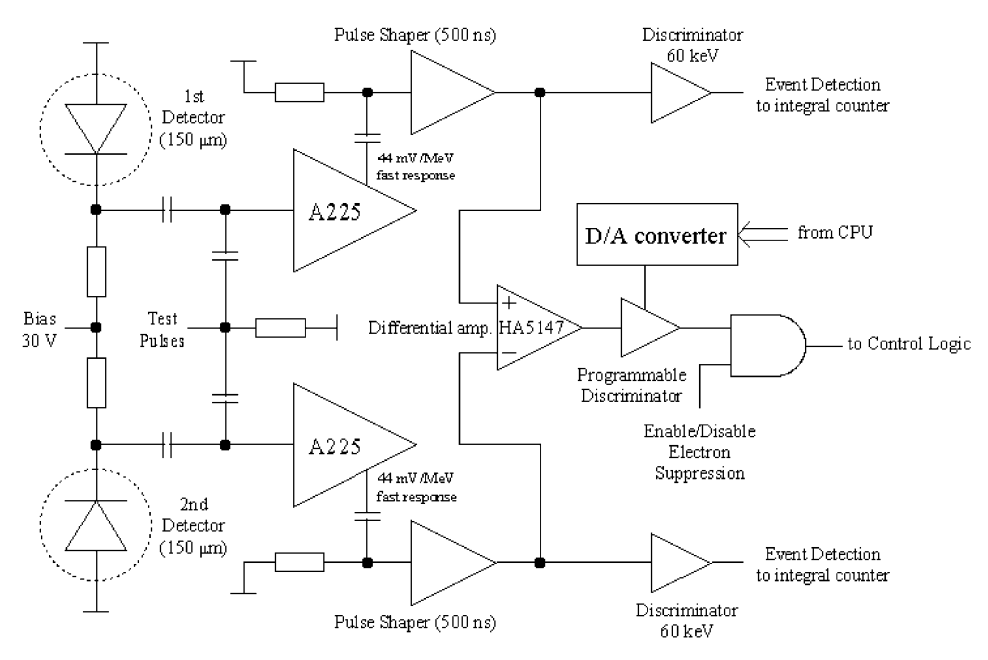


Fig. 7. Block diagram of the electron suppression logic.

Analyser based on an 8 bit Flash Analog-to-Digital converter. Separate ADCs are provided for each of the telescopes. The block diagram of the PHA is shown in Fig. 8. There are two such blocks in the Proton Detector serving the individual telescopes.

Although the energy resolution is very good at the bottom of the range (approx. 200 keV/channel) it is significantly lower at the high end of the spectrum (approx. 50 MeV/channel). This results from the hyperbolic nature of the energy loss (already referred to). However, as a 256-channel resolution is not required for the GPB application, the microprocessor is programmed to sum a preselected number of channels into one channel (the energy limits of which can be flexibly defined) in order to end up with a desired 16 channels. These default science channels are listed in Table 2.

The depth of the PHA channels is 8 bit and, therefore, it is necessary to read the data out every 100 ms to avoid an overflow. As this (basic) time resolution is generally not required, the processor may be used to sum the counts in the selected data channels in order to achieve a particular time resolution (programmable).

The most vulnerable parts of any intelligent, semiconductor based, particle detection system are its microprocessor (CPU) and memory devices, which, as they are VLSI components, are very sensitive to penetrating particle radiation. For GPB/EPM, a radiation hardened CPU was utilised. Although this component is not entirely Latch-Up free, it is rather tolerant to transient upsets (up to 10<sup>8</sup> rad/s) and also remains fully operational up to 10<sup>5</sup> rad total dose.

Special latch-up protection is provided for the entire electronic assembly by the introduction of fast current limiters. These are utilised to protect the CMOS devices from permanent damage resulting from excess current flowing through the silicon substrates due to incident penetrating particles.

# 6. Software design

A key element in the design is the *operating* software that ensures continuous operation. This is based on a real time, multi-tasking Operating System. A low priority task provides continuous

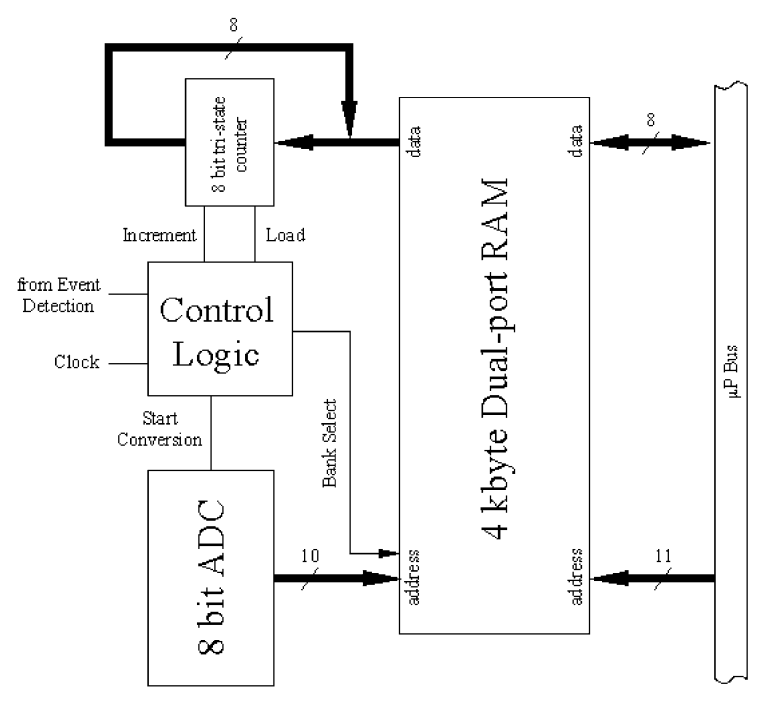


Fig. 8. Block diagram of the PHA.

Table 2 Pre-set channels of the EPM

	A	В	C	D
1	34–40	34–37	34–51	34–51
2	40-48	37-41	52-79	52-79
3	48-57	41-45	79–86	79-120
4	57-68	45-50	86-94	133-148
5	68-81	50-55	94-103	148-165
6	81-96	55-60	103-113	165-183
7	96-114	60-66	113-124	183-203
8	114-135	66–73	124-136	203-226
9	135-160	73-80	136-149	226-251
10	160-190	80-88	149-163	251-279
11	190-225	88–97	163-179	279-310
12	225-266	97-107	179-197	310-345
13	266-315	107-160	197-217	345-383
14	315-373	160-238	217-238	383-425
15	373-442	238-350	238-350	425-472
16	442–525	350-525	350-525	472–525

monitoring of the memory. Since copies of the executable code are stored in physically different memory devices, the SW can correct soft errors in its own system memory based on a majority voting scheme.

Also it is noted that the EPM measurements are under complete software control—so that the processor can adjust all the key measurement parameters during flight (such as the offset; conversion gain; thresholds; energy resolution; time resolution, etc.) using ground commands. Further, an in-flight calibrator allows verification of these various parameters while the instrument is in orbit.

The measurement parameters can be set during calibration to their default values. The onboard SW starts up with these default values but it is possible to modify them during testing using the instrument's 'Debug Mode'.

There are four pre-set channel configurations defined for the EPM, which can be recognised in Table 2. The 'Default Configuration' is labelled A. Also, it is possible to select several pre-defined configurations during flight. In this connection there are several possible time resolutions (such as 3.2, 6.4, 12.8, 25.6 and 51.2 s) and the operator may select any of these by ground command. The default time resolution is 12.8 s (this is driven by the operation of the, onboard, Experiment Control Unit, which is a spacecraft subsystem).

# 7. Ground support equipment/calibration

The Ground Support Equipment (GSE) was used extensively during the Ground Operations phase since, in addition to functional testing, it was employed for the calibration of the instrument at the COSY accelerator in Julich, Germany. The GSE consists of several functional blocks, namely

the: Computer Interface; Control Unit; Power Supply Simulator; Instrument Interface Simulator and the Stimuli Pulse Generator. The set-up adopted when using the EPM with the GSE is shown in Fig. 9.

During calibration, the GSE Stimuli Pulse Generator was calibrated first. This is a high stability precision device that has the capability to

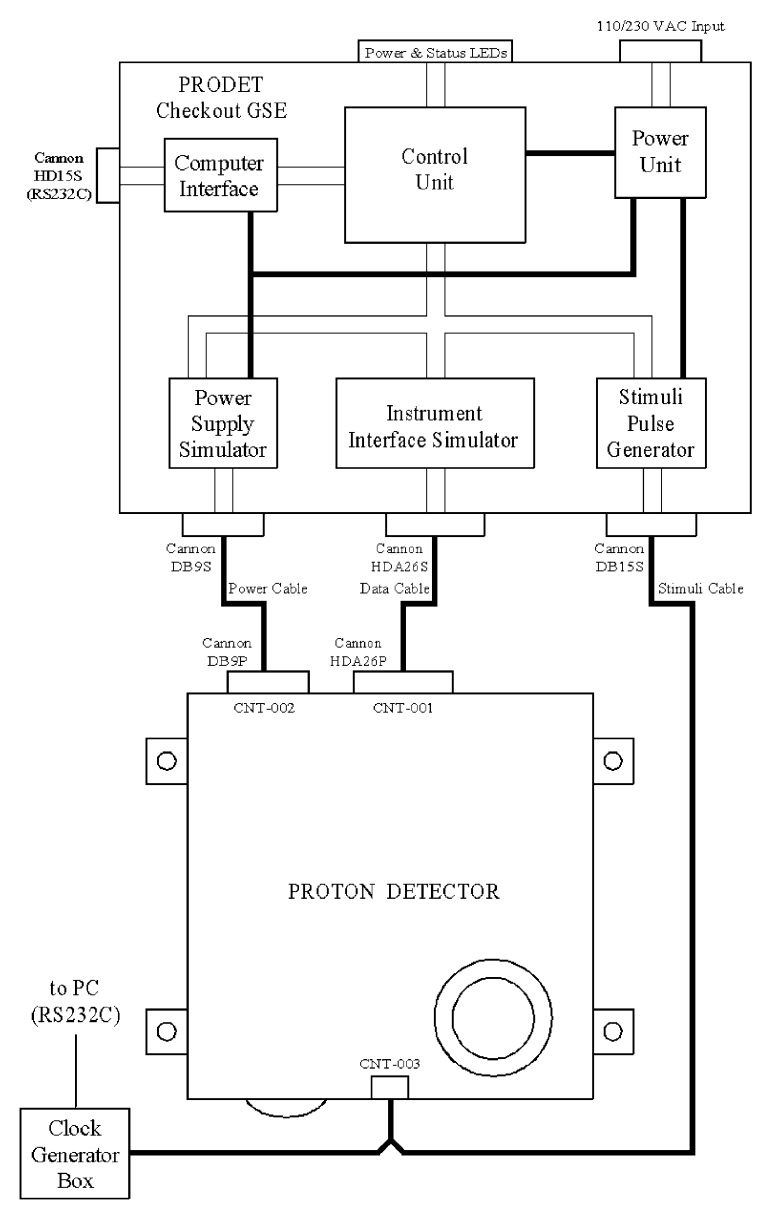
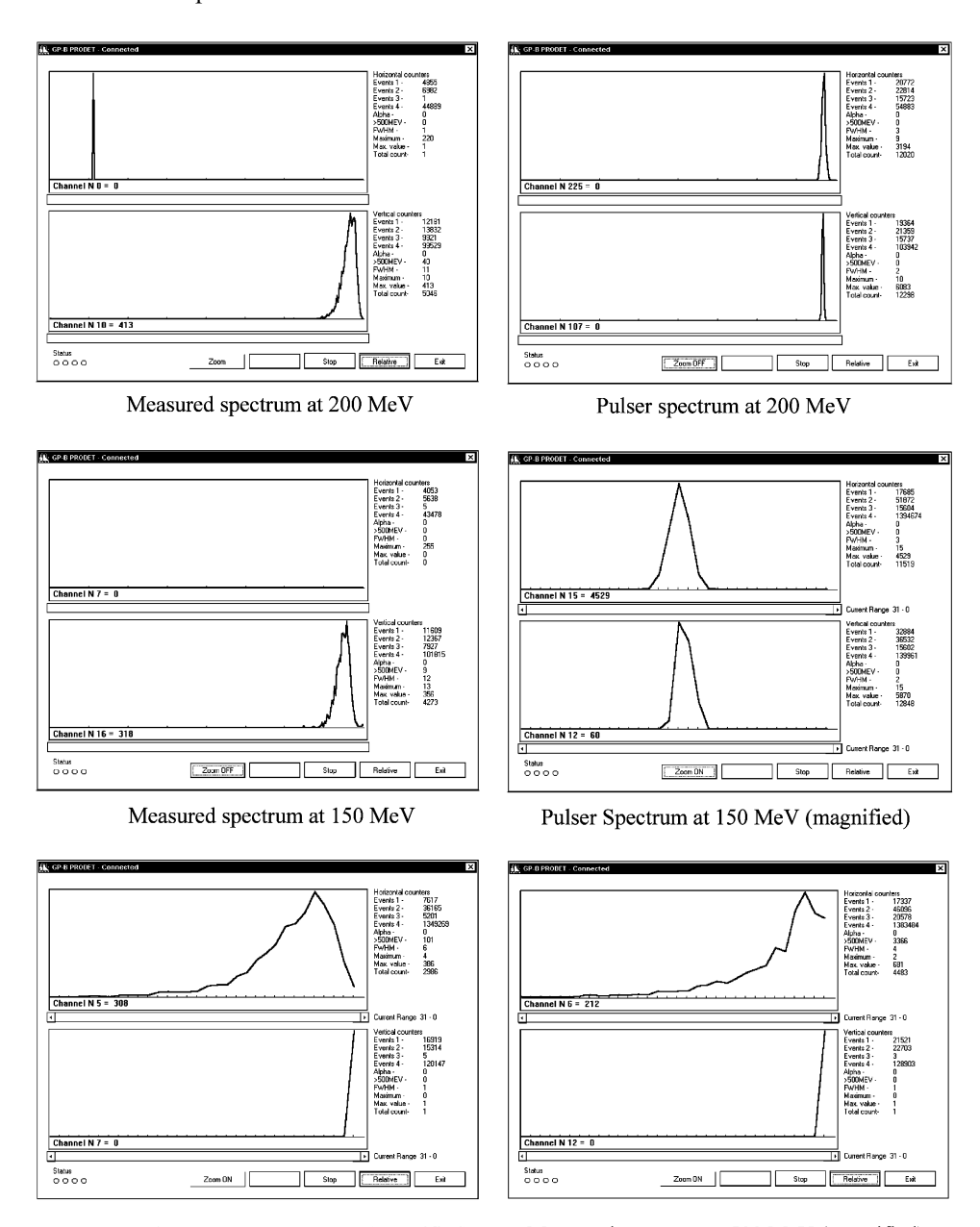


Fig. 9. Setup using the EPM and GSE.

supply a signal to all four detectors in parallel. Thus, the two Telescopes are driven in parallel when external stimuli are used. The Pulser was calibrated separately for both Telescopes at the distinct energies 40, 100, 150, 200, 300 and 500 MeV. The calibrated pulser was then used to

set the thresholds, offsets and gains within the instrument.

Sample data recorded during instrument calibration at the accelerator are shown in Fig. 10. The data given in each spectrum (on the right side) determines the resolution and scale of the data



Measured spectrum at 300 MeV (magnified)

Measured spectrum at 500 MeV (magnified)

Fig. 10. Data collected at the COSY accelerator Julich, Germany, August 1998.

displayed. Such spectra can be conveniently displayed using different full-scale ranges/resolution.

The device can be used (as for GPB) to provide a monitoring function but it can also be flown to obtain high-quality scientific measurements.

# 8. Conclusion

The Energetic Particle Monitor described can provide continuous, reliable operation in the hostile particle environment present along the GPB trajectory.

It uses a unique method of reducing electron contamination to provide pure proton measurements over the, broad, energy range 35–500 MeV.

#### References

- [1] C. Underwood, In-situ radiation effects monitoring on the UoSAT satellites, Proceedings of the Fourth Annual AIAA/USU Conference on Small Satellites, Logan, Utah, USA, August 1990, pp. 27–30.
- [2] J. Feynman, L.W. Armstrong, D. Gibner, S.A. Silvermann, Solar proton events during solar cycles 19, 20 and 21, Sol. Phys. 126 (2) (1990) 385.